

# Robust characterisation of any linear photonic device

Saleh Rahimi-Keshari<sup>1</sup>, Matthew A. Broome<sup>1,2</sup>, Robert Fickler<sup>3,4</sup>,  
Alessandro Fedrizzi<sup>1,2</sup>, Timothy C. Ralph<sup>1</sup>, and Andrew G. White<sup>1,2</sup>

<sup>1</sup>Centre for Engineered Quantum Systems, <sup>2</sup>Centre for Quantum Computer and Communication Technology,  
School of Mathematics and Physics, University of Queensland, Brisbane, QLD 4072, Australia

<sup>3</sup>Quantum Optics, Quantum Nanophysics, Quantum Information, University of Vienna, A-1090, Austria

<sup>4</sup>Institute for Quantum Optics and Quantum Information, Boltzmannngasse 3, Vienna A-1090, Austria

We introduce an efficient method for characterizing the unitary matrix describing a multi-mode linear photonic device. By using readily available single- and two-mode coherent states as probe states and measuring the intensities of the output coherent states, all the moduli and phases of the unitary matrix can be directly measured. We illustrate our method by characterising a  $3 \times 3$  fused-fibre coupler and independently verify the results via non-classical two-photon interference.

PACS numbers:

The art of engineering quantum technologies is to realise arbitrary unitary operators, enabling applications such as efficient quantum simulation [1, 2] and computation [3]. In principle, linear photonic devices can be used to experimentally realise any  $N \times N$  unitary operator [4]: the significant practical challenge is to characterise the device once it is built. A known solution to this challenge is to perform full quantum process tomography of a device using nonclassical lights [5–7] or coherent states [8, 9]. The standard approach however requires the full suite of quantum tools such as  $N$ -mode quantum state preparation and measurement and is—despite progress on more efficient methods such as compressive sensing [10]—relatively slow and not very practical for a large interferometric device.

A more tractable approach starting from the assumption of linearity is to adapt existing methods from classical optics. Since a linear photonic circuit can always be cast as a interferometer with  $(N^2 - N)/2$  beam-splitters [4], it can be fully characterised by embedding it in an external interferometer using a local oscillator. The interferometric stability required is sufficiently challenging in practice that this is rarely done for quantum optics experiments. A recently proposed technique is to use non-classical interference [11] for characterisation [12, 13]: although robust in principle, this technique requires single-photon sources and counters and does not allow full reconstruction of an underlying unitary.

Here we introduce an efficient technique to characterise the unitary matrix of a linear photonic device using standard laser sources and photodetectors—it requires neither interferometric stability nor as-of-yet unavailable pure single photon sources. Our method is robust, cheap, precise, and efficient, requiring only  $2N - 1$  measurement configurations for a  $N$ -path network. We demonstrate our method by characterising an integrated device—a  $3 \times 3$  fused-fibre coupler—and highlight its precision by comparing measured quantum interference patterns with those predicted using the estimated unitary.

An ideal linear photonic network can be represented

as a unitary matrix  $U$  that relates creation operators of the input and output modes

$$b_i^\dagger = \sum_{j=1}^N U_{ij} a_j^\dagger. \quad (1)$$

Generally, the elements of the matrix  $U$  are complex numbers  $U_{ij} = r_{ij} e^{i\theta_{ij}}$ , where  $0 \leq r_{ij} \leq 1$  and  $0 \leq \theta_{ij} < 2\pi$ . For a matrix with  $N^2$  complex entries there are  $2N^2$  parameters to be specified, but due to  $U$  being unitary, we have  $N^2$  constraints  $\sum_i^N U_{ji} U_{ki}^* = \delta_{jk}$ , which reduces the number of free parameters to  $N^2$ . Further, noting that the phases of the basis vectors are not physically significant, we can absorb another  $(2N - 1)$  phases into the basis vectors [14]. Thus, any  $N \times N$  unitary matrix can be decomposed as a product of three unitary matrices  $U = D(\boldsymbol{\mu}) U' D(\boldsymbol{\nu})$ , where  $D(\boldsymbol{\mu}) = \text{diag}(e^{i\mu_1}, e^{i\mu_2}, \dots, e^{i\mu_N})$  and both  $U$  and  $U'$  describe the same physical process. Without loss of generality, we let  $\theta_{1j} = \theta_{j1} = 0$ , for  $j = 1, 2, \dots, N$ , and we are left with  $(N - 1)^2$  free parameters to be determined in the characterisation.

It has been shown that having all the moduli  $r_{ij}$ , where  $r_{ij}^2$  is the probability of detecting a photon at the output port  $i$  when only one single photon was sent to the input port  $j$ , cannot uniquely determine all the phases of the unitary matrix for  $N > 3$  [14, 15]. Therefore, in order to characterise the unitary matrix, we require probe states and measurements that are sensitive to the phases  $\theta_{ij}$ .

One way to achieve that, as shown in [12, 13], is to insert two single photons into different input modes and to record non-classical interference patterns between all combinations of output modes. This method however suffers from the lack of true single-photon sources, is relatively slow as it involves solving nonlinear algebraic equations in terms of phases, and is somewhat circular for applications aiming at multi-photon interference experiments. Our method only requires single- and two-mode coherent states, which are readily available from a laser source with variable input phases. We then simply mea-

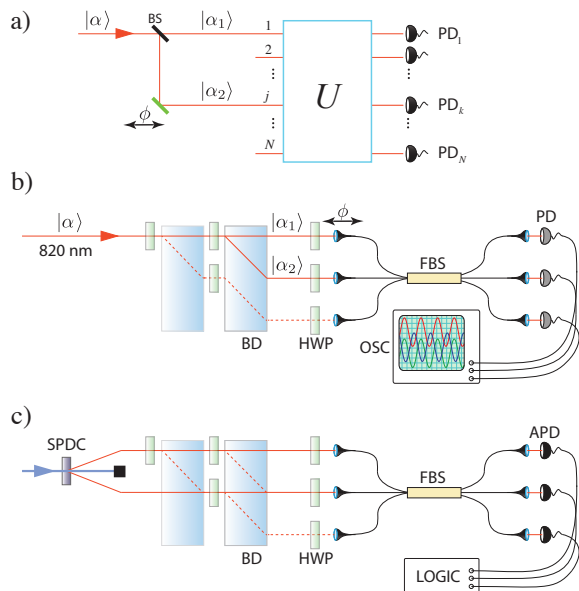


FIG. 1: (a) Conceptual scheme for performing phase-sensitive measurements. Using a 50:50 beam-splitter (BS) and phase shifter ( $\phi$ ) a two-mode coherent state is prepared and sent through the linear photonic network  $U$ . By adjusting the phase and measuring the output intensities with photodetectors (PD), all the phases of matrix  $U$  can be directly measured. (b) Experimental scheme for characterising a passive photonic network. The device under test is a symmetric 3-mode fused-fibre beam-splitter (FBS). Interferometric probe states between pair-wise input combinations are prepared with two polarisation beam displacers (BD), and half-wave plates (HWP). The outputs are monitored with an oscilloscope (OSC) while the phase  $\phi$  is scanned with a motorised translation stage. (c) Experimental schematic for the two-photon non-classical interference experiments. A pair of photons is generated via spontaneous parametric downconversion (SPDC) in a nonlinear beta-barium-borate (BBO) crystal with type-I phase matching to produce polarisation degenerate photons. The individual downconversion modes are steered into the modes of the linear photonic network by a series of beam displacers and half-wave plates. Upon passing through the photonic circuit the photons are detected using avalanche photo-diodes (APD) whose coincident signals are monitored using a commercially available counting logic.

sure the intensities of output coherent states Fig. 1(a). An interesting feature of this method is that it enables us to measure all the nontrivial phases of the unitary directly without solving any algebraic equations. Note that two-mode coherent state with random relative phase has been used to simulate quantum interferences, but not to characterise the unitary matrix [16, 17].

Our method works as follows (details of the algorithm can be found in the Appendix):

1. Send light into the  $N$  input modes individually, and measure the output  $r_{jk}^2$  of all  $k = 1 \dots N$  outputs modes for every input  $j$ . From this, obtain  $r_{jk}$ .

2. Interferometrically prepare pairwise input combinations between input 1 and input  $2 \dots N$ , with a variable phase  $\phi$ . Measure the output intensities of all modes  $k = 1 \dots N$  as a function of  $\phi$ . This yields all non-trivial phases  $\theta_{jk}$ .

We tested our technique by characterising the unitary operation of a single-mode fused fibre-optic  $3 \times 3$  beam-splitter (FBS). The experimental setup is shown in Fig. 1(b). We used a series of polarisation beam displacers and half-wave plates to prepare the input probe states. This allows for phase-stable interferometric measurements and polarisation control on the input of the FBS to ensure each mode receives the same polarisation input. The phase,  $\phi$  was controlled by a motorised micro-translation stage which adjusted the path length difference between two input arms of the interferometer. The outputs were coupled to fast photodiodes and monitored simultaneously on an oscilloscope while the phase was scanned. All characterisation measurements were performed with a  $100 \mu\text{W}$  laser diode with a centre wavelength of 820 nm and a full-width-at-half-maximum bandwidth of 2 nm.

We first measured the nine output intensities for the three individual inputs. We then recorded interference fringes for all possible pair-wise input combinations and fitted sinusoidal curves to the resulting photocurrents to obtain experimental values for  $\theta_{jk}$  (see Appendix for details), see Fig 2. The entire characterisation method was performed 10 times to obtain experimental uncertainties.

From these measurements, we reconstructed the  $3 \times 3$  matrix  $U_{\text{exp}}$ ,

$$U_{\text{exp}} = \begin{pmatrix} 0.424 & 0.519 & 0.495 \\ 0.560 & -0.171 + 0.412i & -0.304 - 0.422i \\ 0.511 & -0.286 - 0.438i & -0.140 + 0.467i \end{pmatrix}. \quad (2)$$

For ideal lossless devices and ideal measurements  $U_{\text{exp}}$  is the unitary matrix describing the linear photonic device; however, due to loss effects this matrix is not unitary. Nevertheless, it can be used to predict the visibilities of non-classical two-photon (or multi-photon) interference which we did to verify our characterisation method [11].

We performed non-classical interference [11] measurements between two-single photons sent into the three combinations of inputs modes and measured the coincidences at the three combinations of outputs, see Fig. 1(c). The visibility of non-classical interference is calculated as  $v = (C_{\text{out}} - C_{\text{in}})/C_{\text{out}}$  where  $C_{\text{out}}$  and  $C_{\text{in}}$  are the coincidence count rates of photon pairs at the outputs of the circuit inside (maximum temporal overlap between photons) and outside (no overlap) the interference dip, respectively. The results are shown in Fig. 3. Note that the discrepancy between the predicted non-classical visibility and those obtained from true two-photon interference is predominantly due to polarisation non-degeneracy between interfering photons inside the FBS.

In principle, as optical losses can be modeled by considering virtual beam-splitters and extra modes associated to them, the matrix  $U_{\text{exp}}$  is a block of a bigger matrix that is unitary. Assuming the loss is equal for different paths connecting specific inputs to outputs and modelling

optical losses as beam-splitters on the input modes our method enables us to obtain the  $6 \times 6$  matrix  $V_{\text{exp}}$  following the algorithm described in the Appendix. If a linear photonic device satisfies this assumption, we would expect  $V_{\text{exp}}$  to be unitary. The matrix  $\mathcal{I}_{\text{exp}} = V_{\text{exp}} V_{\text{exp}}^\dagger$ ,

$$\mathcal{I}_{\text{exp}} = \begin{pmatrix} 1.000 + 0.000i & -0.032 - 0.013i & -0.022 + 0.004i & 0.000 + 0.000i & 0.019 + 0.008i & 0.013 - 0.003i \\ -0.032 + 0.013i & 1.000 + 0.000i & -0.030 + 0.011i & 0.019 - 0.008i & 0.000 + 0.000i & 0.017 - 0.006i \\ -0.022 - 0.004i & -0.030 - 0.011i & 1.000 + 0.000i & 0.013 + 0.003i & 0.018 + 0.007i & 0.000 + 0.000i \\ 0.000 + 0.000i & 0.016 + 0.008i & 0.013 - 0.002i & 1.000 + 0.000i & -0.011 - 0.005i & -0.007 + 0.001i \\ 0.019 - 0.008i & 0.000 + 0.000i & 0.018 - 0.007i & -0.011 + 0.005i & 1.000 + 0.000i & -0.010 + 0.004i \\ 0.013 + 0.003i & 0.017 + 0.006i & 0.000 + 0.000i & -0.007 - 0.001i & -0.010 - 0.004i & 1.000 + 0.000i \end{pmatrix}, \quad (3)$$

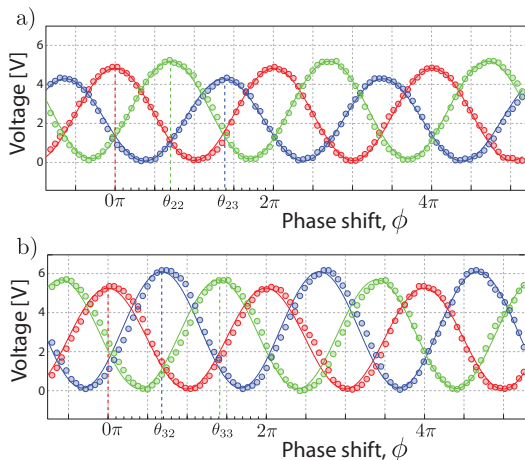


FIG. 2: Representative experimental data for obtaining  $\theta_{jk}$ . a) Injecting coherent light into input modes 1 and 2 of the fibre beam-splitter. The amplitudes of the three output modes (voltage at output photo-diodes) oscillate as the phase  $\phi$  is swept in time. b) Injecting coherent light into input modes 1 and 3. Red, blue and green correspond to output modes 1, 2 and 3 respectively. The circles show measured data and the solid lines are theoretical fits to  $A \cos(\phi - \theta_{jk})$ . After performing this characterisation method 10 separate times the average values for  $\theta_{jk}$  were  $\theta_{22} = 0.6249(65)$ ,  $\theta_{23} = -0.6987(68)$ ,  $\theta_{32} = -0.6844(49)$ ,  $\theta_{33} = 0.5928(81)$ .

has non-zero but very small off-diagonal elements indicating the effect of *path-dependent* loss in the system. The closest unitary matrix to  $V_{\text{exp}}$  can be found by using the polar decomposition  $\tilde{U} = (V_{\text{exp}} V_{\text{exp}}^\dagger)^{-\frac{1}{2}} V_{\text{exp}}$  [18]. The unitary matrix  $\tilde{U}$  does not alter the predicted two-photon interference visibilities shown in 3, however, since the distance  $||[V_{\text{exp}}]_{jk} - \tilde{U}_{jk}||$  is less than the experimental uncertainty of  $[V_{\text{exp}}]_{jk}$  the unitary matrix  $\tilde{U}$  describes our device with a good approximation.

In summary, we have introduced an efficient method for characterising any multi-mode linear photonic device using only single- and two-mode coherent states. One of

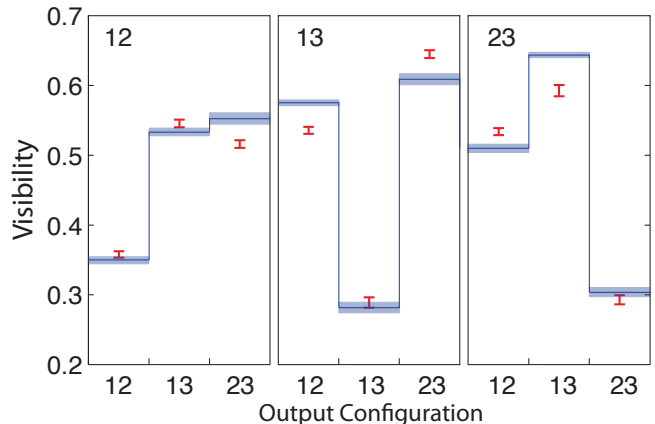


FIG. 3: Two-photon non-classical interference inside a  $3 \times 3$  fused-fibre beam-splitter. a) The red data points bars show the experimental visibilities and the blue lines show the predictions given by the characterisation method. There are three combinations of input modes into which we can launch two photons into the device, likewise for detection, shown by the numbers on the x axes.

the most compelling aspects of our method is its ability to accurately predict quantum dynamics without the need to employ full process tomography or use exotic light sources. Our method therefore substantially simplifies the task of characterisation, in particular, if a large number of optical modes are involved.

As photonic quantum technologies mature beyond small-scale proof-of-principle demonstrations of computation and simulation, there is increasing requirement for improved methods for full tomography, process validation and verification. Areas of direct applicability include the experimental characterisation of large linear waveguide arrays for photonic photon quantum walks [19, 20], especially those built in 3D where current approaches using top-down imaging are not possible [21].

One of the most exciting applications for larger systems pertains to an intermediate model of quantum computation—namely, that of BOSONSAMPLING [2]. In

this model one must be able to efficiently characterise large linear optical networks to obtain the scattering probabilities of multi-photon processes. Importantly, the characterisation must be sufficiently accurate to overlap with true non-classical interference experiments.

### Acknowledgements

We thank Shahla Nikbakht for discussions. This work was supported in part by: the Australian Research Council's Federation Fellow program (FF0668810), Centre for Engineered Quantum Systems (CE110001013), Centre for Quantum Computation and Communication Technology (CE110001027), and the SFB program W1210-2 (Vienna Doctoral Program on Complex Quantum Systems - CoQuS) of the Austrian Science Fund (FWF); and the University of Queensland Vice-Chancellor's Senior Research Fellowship program.

### Appendix

In practice, there is no lossless photonic device, meaning that the matrix relating creation operators of the output modes to those of input (Eq. 1) is not unitary. For linear photonic devices the loss effects can be taken into account by considering some virtual beam-splitters and additional modes. Assuming the loss is equal from one-

input mode to all output modes, we model losses by adding virtual beam-splitters with reflectivity  $\eta_j$  ( $0 \leq \eta_j \leq 1$ ) to each input of a unitary matrix  $U$ , with the resulting  $2N$ -by- $2N$  unitary matrix referred to as  $V$ . Here we describe our method for characterising  $V$  as a unitary matrix.

The first step towards characterization of  $V$  is to find all the moduli of the matrix  $V$ . Using Eq. (1), the output amplitudes of a general  $N$ -mode input coherent state  $|\alpha_1, \alpha_2, \dots, \alpha_N\rangle$  are given by

$$\beta_k = \sum_{j=1}^N V_{jk} \alpha_j. \quad (4)$$

We can thus send a coherent state with known intensity  $I$  to input port  $j$ , where all other input modes are in vacuum state, and measure the intensity from all output ports simultaneously

$$I_k = I (\eta_j r_{jk})^2, \quad k = 1, 2, \dots, N. \quad (5)$$

We also have

$$(\eta_j)^2 = \frac{1}{I} \sum_{k=1}^N I_k. \quad (6)$$

Thus using equations (5) and (6) for  $j = 1, \dots, N$  all the moduli of the matrix  $V$  can be obtained,

$$V = \begin{pmatrix} \eta_1 r_{11} & \eta_1 r_{12} & \eta_1 r_{13} & \dots & \eta_1 r_{1N} & \sqrt{1-\eta_1^2} & 0 & 0 \\ \eta_2 r_{21} & \eta_2 r_{22} e^{i\theta_{22}} & \eta_2 r_{23} e^{i\theta_{23}} & \vdots & \vdots & 0 & \sqrt{1-\eta_2^2} & \vdots \\ \vdots & \vdots & \vdots & \ddots & \vdots & \vdots & \vdots & \ddots \\ \eta_N r_{N1} & \eta_N r_{N2} e^{i\theta_{N2}} & \dots & \dots & \eta_N r_{NN} e^{i\theta_{NN}} & 0 & 0 & \sqrt{1-\eta_N^2} \\ -\sqrt{1-\eta_1^2} r_{11} & -\sqrt{1-\eta_1^2} r_{12} & -\sqrt{1-\eta_1^2} r_{13} & \dots & -\sqrt{1-\eta_1^2} r_{1N} & \eta_1 & 0 & 0 \\ -\sqrt{1-\eta_2^2} r_{21} & -\sqrt{1-\eta_2^2} r_{22} e^{i\theta_{22}} & -\sqrt{1-\eta_2^2} r_{23} e^{i\theta_{23}} & \vdots & \vdots & 0 & \eta_2 & \vdots \\ \vdots & \vdots & \vdots & \ddots & \vdots & \vdots & \vdots & \ddots \\ -\sqrt{1-\eta_N^2} r_{N1} & -\sqrt{1-\eta_N^2} r_{N2} e^{i\theta_{N2}} & \dots & \dots & -\sqrt{1-\eta_N^2} r_{NN} e^{i\theta_{NN}} & 0 & 0 & \dots & \eta_N \end{pmatrix}.$$

The next step is to measure all nontrivial phases using two-mode coherent states. We send a coherent state  $|\alpha\rangle$  to a 50:50 beam-splitter and use a phase shifter to control the relative phase between the output states  $|\alpha_1\rangle$  and  $|\alpha_2\rangle$  with the same intensity  $I$ ; see Fig. 1(a). We send  $|\alpha_1\rangle$  to input 1 and  $|\alpha_2\rangle$  to input port  $j$ , sweep the relative phase  $\phi$  from 0 to  $2\pi$  and measure the intensities of the

output coherent states

$$I_k = I |V_{1k} + V_{jk} e^{i\phi}|^2. \quad (7)$$

Since all elements in the first row and the first column

are real, the above equation becomes

$$\begin{aligned} I_k &= I \left| \eta_1 r_{1k} + \eta_j r_{jk} e^{i(\phi + \theta_{jk})} \right|^2 \\ &= I \left[ (\eta_1 r_{1k})^2 + (\eta_j r_{jk})^2 + 2\eta_1 \eta_j r_{1k} r_{jk} \cos(\phi + \theta_{jk}) \right]. \end{aligned} \quad (8)$$

In order to obtain the phases  $\theta_{jk}$  the relative phase  $\phi$  between input coherent states must be known. To determine  $\phi$  we change the phase of  $|\alpha_2\rangle$  and measure intensity of coherent state at the first output port

$$I_1 = I \left[ (\eta_1 r_{11})^2 + (\eta_j r_{j1})^2 + 2\eta_1 \eta_j r_{11} r_{j1} \cos(\phi) \right]. \quad (9)$$

When this quantity attains its maximum value we have  $\phi = 0$ , and for minimum value  $\phi = \pi$ . Thus we can calibrate and adjust the relative phase  $\phi$  to be any arbitrary value between zero and  $2\pi$ , by using  $I_1$  as the reference. Having this capability, we can tune  $\phi$  such that  $I_k$  be maximum and using Eq. (8) the unknown phases can be found as

$$\theta_{jk} = 2\pi - \phi. \quad (10)$$

Therefore, by repeating this procedure for  $j = 2, \dots, N$  all the nontrivial phases of the matrix  $V$  can be directly measured.

- 
- [1] B. Lanyon, J. Whitfield, G. Gillett, M. Goggin, M. Almeida, I. Kassal, J. Biamonte, M. Mohseni, B. Powell, M. Barbieri, et al., *Nature Chemistry* **2**, 106 (2010).  
 [2] S. Aaronson and A. Arkhipov, *Proc. ACM Symposium on Theory of Computing*, San Jose, CA pp. 333-342 (2011).  
 [3] B. P. Lanyon, T. J. Weinhold, N. K. Langford, M. Barbieri, D. F. V. James, A. Gilchrist, and A. G. White, *Phys. Rev. Lett.* **99**, 250505 (2007).

- [4] M. Reck, A. Zeilinger, H. Bernstein, and P. Bertani, *Phys. Rev. Lett.* **73**, 58 (1994).  
 [5] J. L. O'Brien, G. J. Pryde, A. Gilchrist, D. F. V. James, N. K. Langford, T. C. Ralph, and A. G. White, *Phys. Rev. Lett.* **93**, 080502 (2004).  
 [6] A. M. Childs, I. L. Chuang, and D. W. Leung, *Phys. Rev. Lett.* **64**, 012314 (2001).  
 [7] M. W. Mitchell, C. W. Ellenor, S. Schneider, and A. M. Steinberg, *Phys. Rev. Lett.* **91**, 120402 (2003).  
 [8] M. Lobino, D. Korystov, C. Kupchak, E. Figueroa, B. C. Sanders, and A. I. Lvovsky, *Science* **322**, 563 (2008).  
 [9] S. Rahimi-Keshari, A. Scherer, A. Mann, A. T. Reza-khani, A. I. Lvovsky, and B. C. Sanders, *New J. Phys.* **13**, 013006 (2011).  
 [10] A. Shabani, R. L. Kosut, M. Mohseni, H. Rabitz, M. A. Broome, M. P. Almeida, A. Fedrizzi, and A. G. White, *Phys. Rev. Lett.* **106**, 100401 (2011).  
 [11] C. K. Hong, Z. Y. Ou, and L. Mandel, *Phys. Rev. Lett.* **59**, 2044 (1987).  
 [12] A. Peruzzo, A. Laing, A. Politi, T. Rudolph, and J. L. O'Brien, *Nature Communications* **2**, 224 (2011).  
 [13] A. Laing and J. L. O'Brien, arXiv:1208.2868 (2012).  
 [14] A. Peres, *Nucl. Phys. B* **6**, 243 (1989).  
 [15] H. J. Bernstein, *J. Math. Phys.* **15**, 1677 (1974).  
 [16] Y. Bromberg, Y. Lahini, R. Morandotti, and Y. Silberberg, *Phys. Rev. Lett.* **102**, 253904 (2009).  
 [17] R. Keil, A. Szameit, F. Dreisow, M. Heinrich, S. Nolte, and A. Tünnermann, *Phys. Rev. A* **81**, 023834 (2010).  
 [18] K. Fan and A. J. Hoffman, *Proc. Amer. Math. Soc.* **6**, 11 (1955).  
 [19] A. Peruzzo, M. Lobino, J. Matthews, N. Matsuda, A. Politi, K. Poullos, X. Zhou, Y. Lahini, N. Ismail, K. Wörhoff, et al., *Science* **329**, 1500 (2010).  
 [20] L. Sansoni, F. Sciarrino, G. Vallone, P. Mataloni, A. Crespi, R. Ramponi, and R. Osellame, *Phys. Rev. Lett.* **108**, 10502 (2012).  
 [21] J. O. Owens, M. A. Broome, D. N. Biggerstaff, M. E. Goggin, A. Fedrizzi, T. Linjordet, M. Ams, G. D. Marshall, J. Twamley, M. J. Withford, et al., *New J. Phys.* **13**, 075003 (2011).